Am J Cancer Res 2023;13(4):1471-1485
www.ajcr.us /ISSN:2156-6976/ajcr0148392

Original Article

Somatic-to-primordial germ cell-like transformation is critical in tumor initiation of mouse breast tumor 4T1 cells

Zhan Ma[1,3*], Fengyu Zhang[1*], Aiping Liu[1*], Huikuan Lin[2], Chunfang Liu[1]

[1]Department of Laboratory Medicine, Huashan Hospital, Shanghai Medical College, Fudan University, Shanghai 200040, China; [2]Department of Cancer Biology, Wake Forest University School of Medicine, Winston-Salem, NC 27157, USA; [3]Department of Laboratory Medicine, Shanghai Children's Hospital, Shanghai Jiao Tong University, Shanghai 200040, China. [*]Equal contributors.

Received December 11, 2022; Accepted February 16, 2023; Epub April 15, 2023; Published April 30, 2023

Abstract: It has been proposed that tumorigenicity was an intrinsic feature of embryonic/germ cell developmental axis as well as embryonic/germ cell-related genes play a crucial role in tumorigenicity. Our previous studies indicated that primordial germ cell (PGC)-like potential could be reactivated in tumorigenesis. In this study, 4T1, 168FARN and 67NR cells which originated from the same mouse breast cancer were studied and the results indicated that the acquisition of embryonic/germ cell-like state is essential for tumorigenicity. We further demonstrated that somatic to PGC-like transformation (SPLT) was activated in 4T1 cells and that inhibition of PGC-like cell formation by depleting pluripotency and/or PGC specification-related genes markedly repressed SPLT and the tumorigenicity. Collectively, our findings reveal that tumorigenicity is linked to the acquisition of PGC-like state through SPLT in 4T1 cells, providing new insight into deeper understanding the biological nature of tumors and novel therapeutical strategies for cancer targeting.

Keywords: Tumor initiation, germ cell traits of tumors, primordial germ cell-like tumor cells, somatic to primordial germ cell-like transformation, embryonic/germ cell hypothesis of tumor, breast cancer

Introduction

It is still under debate which phenotype is a driving force in tumor malignant behaviors, such as tumorigenicity. Of note is that embryonal/gametogenesis hypothesis of tumors was postulated at the beginning of tumors identified, which stated that tumors arise from germ cells (missing germ cells or reobtaining the embryonic/germ cell fate of somatic cells) based on the striking similarities between carcinogenesis and embryonic/germ cell development [1-4]. Intriguingly, it has been proposed that tumorigenicity is an intrinsic feature of embryonic/germ cell developmental axis, such as blastomeres, embryonic stem (ES) cells, and early primordial germ cells (PGCs) as well as induced embryonic state-like cells, such as parthenogenesis activation of oocytes, embryonic germ cells (EGCs) and induced pluripotent stem cells (iPS cells) [5-10]. This model postulates that if cells acquiring ES cell or early PGC features occurred in somatic tissues through mechanisms yet to be discovered, tumors might be caused.

More recently, it became increasingly clear that tumor development is highly similar to embryonic/germ cell development in terms of marker expression, pathways involved, behaviors, and immune escape [11-23]. Notably, genes related to embryonic/germ cell developmental axis are essential for tumor formation and progression. In addition to those classical oncogenes and tumor suppressor genes, such as Ras, c-Myc, Rb, p53, and PI3K, which are also known to serve as master regulators in reprograming or embryonic/germ cell development [15, 16, 19, 22, 24-27]. Of note is that our previous studies showed that embryonic/germ cell-like cells appeared in various types of tumor cells, from PGC-like cells, oocyte-like cells to blastomere-

like cells which are associated with tumor formation, liver metastasis, drug resistance and somatic embryo-like life cycle [17, 19, 28-32], providing the possibly cellular basis for the embryonal/gametogenesis-related hypothesis of tumors. Moreover, the activation of embryonic/germ cell-like cell formation appeared in somatic tumor cells can be induced by either chemical carcinogen (3-methyl-cholanthrene, 3-MCA) or p53 deficiency [18, 28]. Therefore, we postulated that somatic to embryonic/germ cell-like state transformation might be a driving force in tumor initiation. In this study, we revealed that somatic to PGC-like transformation (SPLT) is essential for tumorigenicity of mouse breast cancer 4T1 cells.

Materials and methods

Ethics statement

Our animal experiments were carried out in compliance with the American Veterinary Medical Association (AVMA) Guidelines for the Euthanasia of Animals (2020). All animal experiments were approved by with the Institutional Animal Care and Use Committee of Fudan University (approval number: 2019JS-073).

Cell culture

The 168FARN (obtained from Dr. Kounosuke Watabe), 67NR (obtained from Dr. Kounosuke Watabe) and 4T1 (from ATCC cell) cell lines originated from the same breast tumors of BALB/c mice. Transformed bone marrow-derived cells-7 (TBMDCs-7) and TBMDCs-2 were generated from bone-marrow of $p53^{+/+}$ and $p53^{-/-}$ mice respectively and then underwent carcinogenesis by treatment with 3-methyl-cholanthrene (3-MCA) in vitro [19]. For all the cell culture, high-glucose Dulbecco's modified Eagle's medium (DMEM, Hyclone) with 10% fetal bovine serum (FBS; Sigma), 1% L-glutamine and 37°C with 5% CO_2 were used.

Real-time PCR analysis

RNA was obtained from various cells with Trizol reagent (Invitrogen) according to the manufacturer's protocol followed by reverse transcription to cDNA with a reverse transcription kit (Invitrogen). Real-time PCR of the cDNA was performed with the SYBR Green PCR Master Mix Kit (Applied Biosystems). Primers were shown in our previous study [19] and the Table S1.

Alkaline phosphatase staining

Cultures were fixed using 4% paraformaldehyde in PBS for 4 min, washed twice using a Tris-HCl (pH = 8.2) buffer solution and then incubated with AP kit (Vector Laboratory) overnight at room temperature.

Drug treatment

4T1 cells were treated with DMSO or DMH2 (3 μM, 6 μM or 8 μM) for 24 h and 48 h respectively and the protein expression was detected with WB. 4T1 cultures (1×10^5 cells) were treated with DMH2 (8 μM) for 12 h, 24 h and 48 h respectively and the mRNA levels at the different time point were detected. After treatment with DMH2 (8 μM) for 48 h, the 4T1 cells were incubated in normal medium for 12 h, 24 h or 48 h and the mRNA levels at the different time points were detected. The 4T1 cultures treated with DMSO or DMH2 for 48 h were injected into mice (n = 5) for tumor development. To analyze the crucial role of BMP/Smad pathway, 4T1 cells were treated with PBS or LDN193189 2HCl (BMP type I receptor blocking agent [33], 2 μM, 4 μM, 6 μM or 8 μM) for 48 h respectively and then stained with crystal violet.

Antibody

The primary antibodies used in the study included anti-Oct4 (ab184665, Abcam), anti-Sox2 (MAB2018R-100, R&D), anti-Nanos3 (ab-70001, Abcam), anti-Stellar (Invitrogen, PA5-34601), anti-PRDM14 (ab187881, Abcam), anti-DDX4 (ab27591, Abcam), anti-DAZL (NB100-2437, Novus biologicals), anti-Smad2 (ab33-875, Abcam), anti-Acvr1 (ab155981, Abcam), anti-Smad1 (ab33902, Abcam), anti-Smad5 (ab92698, Abcam), anti-Smad4 (ab40759, Abcam).

Immunofluorescence

Cultures were incubated in chamber slide for 24 h and then fixed with 4% paraformaldehyde and stained with several primary antibodies, including anti-Oct4 (1:400), anti-Stellar (1:200; rabbit; AbCam), anti-DAZL (1:300) or anti-DDX-4arom (1:200), washed and then incubated with secondary antibodies conjugated fluores-

cent dye (Alexa Fluor 488 or 555). Cell nuclei were stained with 4, 6-diamidino-2-phenylindole (DAPI; Invitrogen).

Deletion of genes with CRISPR-Cas9 technology

The CRISPR/Cas9 (Addgene, plasmid ID: 48138) and mouse sgRNA-RFP (Sigma) plasmids were used to knockout indicated genes while the guide empty vector (Sigma) was used to serve as the control. X-tremeGENE9 DNA transection Reagent (Roche, 20 μl) and Opti-MEM medium (Gibco, 500 μl) were mixed for 5 min, incubated with 6 μg of lentivirus packaging plasmid (Lentivirus Packaging Vectors L00002M, beyotime) and 6 μg of CRISPR/Cas9 (Addgene, plasmid ID: 48138) for 25 min at room temperature, and then these mixtures were added to HEK293T cells with 9.5 ml Opti-MEM medium. Replace the medium with DMEM containing 10% fetal bovine serum (FBS; Sigma). The medium with the viruses in HEK293T cells was collected after cultured for 24 h and 48 h respectively, filtrated with a 0.45 μm Steri-Flip filter (Millipore), mixed with 20% fresh culture medium containing 7 μg/ml polybrene and then used to transfected 4T1 or 168FARN cells for 4 h. After infected twice with medium with virus and then cultured with normal 10% fresh medium for 48 h, the 4T1 or 168FARN cultures were treated with 4 μg/ml blasticidin for 5 days to obtain the 4T1-Cas9 or 168FARN-Cas9 cells. Then transfected indicated sgRNA (Sigma, Table S2) or guide plasmid (Sigma) to 4T1-Cas9 or 168FARN-Cas9 cells with the same protocol and treated with 5 μg/ml puromycin for 5 days and then isolated single clone with 96-well plates. DNA sequencing and western blot was performed to select the knockout cell clones. The sequencing primer and results of the knockout cells and sgRNA information were provided in Tables S3, S4 and our previous study [19].

Western blotting

Cultures were collected, washed with ice-cold phosphate-buffered saline (PBS), and lysed in 0.5 ml ice-cold radioimmunoprecipitation (RIPA) buffer protease/phosphatase inhibitors for 20 min on ice. Protein was harvested after centrifugation and then boiled in Laemmli buffer for 15 minutes at 4°C. Proteins were resolved by SDS-PAGE and transferred onto a 0.45 mm nitrocellulose membrane (Millipore). Membranes were blocked in 5% milk for 2 h, incubated overnight at 4°C with indicated primary antibody, and then incubated with secondary antibody. Bound antibodies were visualized using and then detected with Imaging System (ChemiScope 6000).

Xenograft animal experiments

All animal experiments were performed in accordance with the National Institutes of Health Guide for the Care. For comparing the tumorigenicity, the 4T1 (5×10^5), 168FARN (5×10^5), 67NR (5×10^5) cells, 4T1 treatment with DMSO or DMH2 as well as the sorted Stellar$^+$ (100 cells) and Stellar$^-$ (100 cells) from 4T1 cells were subcutaneously grafted into 5 BALB/c mice, respectively. For analyzing the roles of the indicated genes, the 4T1 cells knocked out with Oct4, Sox2, Nanog, PRDM14, DDX4, DAZL, Acvr1, Smad1, Smad5 or Blimp1 with CRISPR-Cas9 technology and the 4T1 control cells were subcutaneously grafted into 10 BALB/c mice, respectively. The time of tumor initiation was recorded. The mice were sacrificed with 60% CO_2 for 5 min after the ending of experiments. All animal studies according to protocols approved by the Laboratory Animal Committee of Fudan University and handled with care and euthanized humanely during the experiment.

Cell sorting with FACS

The 4T1 cell cultures were collected by trypsinization, incubated with the antibody against Stellar for 1 h on ice, stained with secondary antibody conjugated to Alexa Fluor488, and then sorted with the flow cytometry sorter.

Statistical analysis

Statistical analysis was performed with GraphPad Prism version 6.0 (San Diego, CA, USA). Between distinct groups. Unpaired t test with Welch's correction and Mann Whitney test were used to calculate the difference of gene expression, the formation efficiency of AP-positive cells or the percentage of AP$^+$ PGC-like cells among distinct groups. Kaplan-Meier curves were used to analyze overall survival for each of the genes and test groups. A *P*-value with < 0.05 was considered statistically significant. All experiments were repeated at least

three times. $P < 0.05$ were considered as statistically significant.

Results

Correlation between embryonic/germ cell-like cell formation and tumor initiation

The isogenic cell subpopulations from the same mouse mammary tumor 4T1, 168FARN and 67NR cells were firstly used to investigate which phenotypic properties is essential for tumorigenicity. Our in vivo animal experiments revealed that the three tumor cells had a marked difference in tumorigenicity (**Figure 1A**). The mice injected with 4T1 cells formed tumors quickly (**Figure 1A**) and developed metastasis [19]. Compared to 4T1 cells, 168FARN cells delayed tumor initiation (**Figure 1A**) and failed to form obvious metastasis [19]. Although 4T1 and 168FARN cells were different in tumor onset, but their tumor growth rate in vivo was similar (**Figure 1A**). However, the mice injected with 67NR cells failed to give rise to tumor 6 months after subcutaneous injection (**Figure 1A**).

The results of DNA and RNA sequencing showed that all three cell lines underwent massive changes in gene sequence and expression (**Figures 1B** and S1, S2, S3, S4, S5). Considering the fact that the three cell lines also showed a distinct difference in gene expression related to tumors, we postulated that their difference in tumorigenicity possibly attributes to a core phenotypic trait induced by a serial of gene changes. To validate our concept that the embryonic/germ cell state might be the core phenotype, we investigated the difference of the three isogenic cells in embryonic/germ cell traits. Interestingly, the ratio of a subpopulation of cells positive for alkaline phosphatase (AP) staining, a marker of embryonic stem cells and early germ cells [34] was significantly distinct in the three cancer cell cultures (**Figure 1C**, **1D**). The AP^+ cells were round in 4T1 cultures (**Figure 1C**), resembling the PGCs in shape which have the ability to drive tumor and metastasis [19]. In 168FARN cultures, AP^+ cells often formed tightly clusters which were closer to ES cell clones in morphology which could cause tumor but fail to drive metastasis (**Figure 1C**). Although there are several gene mutations appeared in the cells (Figure S1), neither PGC-like nor ES-like state was observed in 67NR cultures (**Figure 1C**, **1D**), consistent with their low tumorigenicity [35].

The results of qRT-PCR and Western blot (WB) assays further confirmed the difference in embryonic/germ cell-like cell formation among 4T1, 168FARN and 67NR cell cultures. Compared with 168FARN cell cultures, 4T1 cell cultures displayed much higher expression in genes critical for PGC-like state [34] (**Figure 1E**, **1F**), such as Stellar, Nanos3 and Blimp1, possibly linking to metastatic ability. However, the Sox2 gene was amplified in DNA sequencing analysis (Table S5) and highly expressed in 168FARN cells (**Figure 1E**, **1F**), which might promote the embryonic cell-like state but inhibit PGC-like state [34]. The data of WB showed that some embryonic/germ cell-related genes were also activated in 67NR cells (**Figure 1E**), raising the possibility that tumorigenicity is not caused by single ES/PGC-related gene instead is an outcome of ES/PGC-like state re-obtaining through a gene network operated together. The findings indicated that the ability of AP^+ embryonic/germ cell-like cell formation is positively correlated with tumorigenicity among the three cell lines as well as the PGC-like rather than embryonic cell-like properties link to metastatic ability [19].

The similarly positive correlation between the ability of embryonic/germ cell-like cell formation [19] and tumorigenicity was also observed in transformed bone marrow-derived cells (TBMDCs-2 and TBMDCs-7) (**Figure 1G-I**). Collectively, one of the most intriguing possibilities is that obtaining the ability of embryonic/germ-cell formation might be a driving force in tumorigenicity.

Activation of somatic cell-to-PGC like transformation (SPLT) in 4T1 cells

The studies of iPS cells provided direct evidence for the reprogramming in somatic cells and validated that the reobtaining of the ES-like state in somatic cells could confer tumorigenicity [35]. Because numerous studies showed that embryonic state is essential for tumorigenicity [5, 9, 35], we mainly focused on whether obtaining PGC-like properties plays a crucial role in tumorigenicity in a given tumor cell line, 4T1 cells. In essence, the normal PGCs are unipotent and destinated to develop into oocytes/sperms [34]. In order to further con-

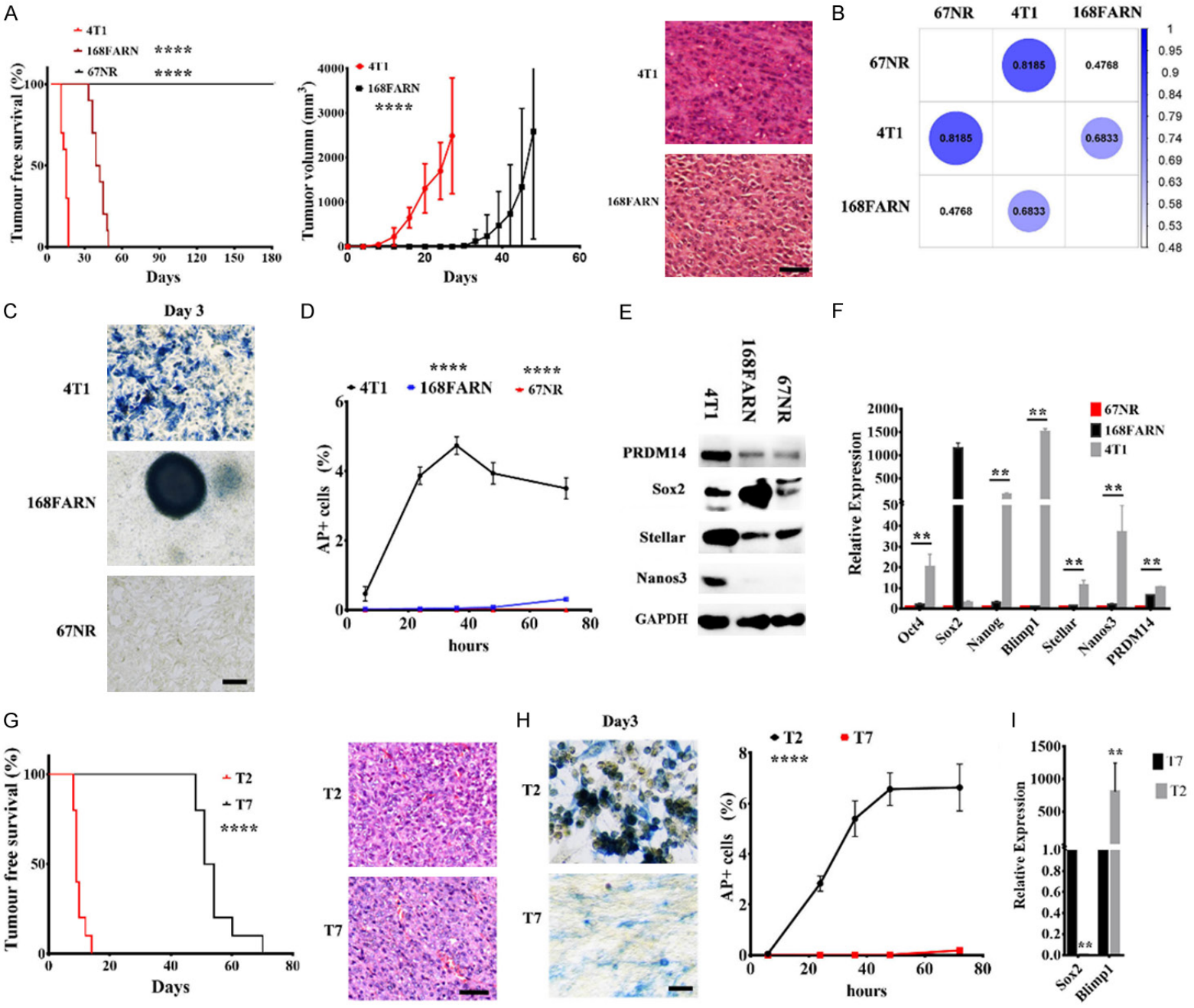
A
4T1
168FARN
67NR
****
****
Tumour free survival (%)
Days
Tumuor volumn (mm3)
B
67NR
4T1
168FARN
0.8185
0.4768
0.6833
C
Day 3
4T1
168FARN
67NR
D
AP+ cells (%)
hours
E
PRDM14
Sox2
Stellar
Nanos3
GAPDH
F
Relative Expression
Oct4
Sox2
Nanog
Blimp1
Stellar
Nanos3
PRDM14
G
T2
T7
H
Day3
I
Relative Expression
Sox2
Blimp1

Figure 1. Embryonic/germ cell-like cell formation associated with tumor initiation. (A) The tumor-free survival curve showed the difference of 4T1, 168FARN and 67NR cells in tumor initiation potential (left). Tumor initiation and growth curve of 4T1 and 168FARN cells (middle). Bright field image of tumor tissue section with HE staining of 4T1 and 168FARN cells (right). (B) DNA sequencing showed the correlation of genetic changes among the 4T1, 168FARN and 67NR cultures. (C) Bright field image showed AP staining in 4T1, 168FARN and 467NR cultures. (D) The plot showed the formation efficiency of AP-positive cells in 4T1, 168FARN and 67NR cultures at different time points. (E) WB results of indicated proteins in 4T1, 168FARN and 67NR cultures. (F) qRT-PCR showed the expression of indicated genes in 4T1, 168FARN and 67NR cultures. (G) The tumor-free survival curve showed the difference of TBMDCs-2 (T2) and TBMDCs-7 (T7) in tumor initiation potential (left). Bright field image of tumor tissue section with HE staining of TBMDCs-2 (T2) and TBMDCs-7 (T7) in mice (right). (H) Bright field image showed AP staining in TBMDCs-2 (T2) and TBMDCs-7 (T7) cultures. The plot showed the formation efficiency of AP-positive cells in TBMDCs-2 (T2) and TBMDCs-7 (T7) cultures at different time points. (I) qRT-PCR showed the expression of indicated genes in T7 and T2 cultures. Scale bar = 50 μm (A, C, H). $^{**}P < 0.01$, $^{****}P < 0.0001$.

firm the similarities between PGC-like cells and natural PGCs, we analyzed the development of PGC-like cells along with germ cell maturation in morphology and marker expression. Round-shaped cells with varied size and positive for AP staining could be observed in 4T1 cells, including PGC-like cells, post-migratory PGC-like cells, and oogonia-like cells, however, the late oocyte-like cells and blastomere-like structures were barely observed in normal culture (**Figure 2A**, **2B**), which required certain culture conditions.

Of note is that the PGCs can return to EGCs and then give rise to somatic cells under certain conditions (e.g. *PTEN* deletion or *TP53* deletion), thereby providing the basis for spontaneous testis teratomas developed in the animal model with *Pten* or *TP53* deficiency [8, 34]. It is possible that the PGC-like cells could return to somatic state through PGC-EGC-somatic cell-like pathway rather than undergoing further development along with germ cell maturation and parthenogenetic activation in 4T1 cultures. To investigate whether PGC-like cells produce somatic tumor cells, we then isolated the Stellar$^+$ (a marker of PGCs, represent PGC-like cells) with FACS analysis in 4T1 cultures. Compared to Stellar cells, the Stellar$^+$ cells displayed the high expression of the genes related to PGC-like state (**Figure 2C**). As expected, the Stellar$^+$ cells switched back to somatic cells after culture instead to the oocyte-like cells (**Figure 2D**). Of note, the stellar cells (represent somatic tumor-like cells) isolated from 4T1 cultures with FACS could generate PGC-like cells (**Figure 2D**). In addition, both 100 Stellar$^+$ cells and 100 Stellar cells of 4T1 cultures injected to mice displayed similar tumorigenicity potential (**Figure 2E**). Consistent with this result, the AP$^+$ round-shaped cells and the AP$^-$ somatic-shaped cells also could switch mutually, even at single cell level (**Figure 2F**). After 12 h culture, almost all cells showed somatic morphology and low AP expression in 4T1 single cell culture (**Figure 2F**). With the long-term culture for a month, AP$^+$ round cells appeared and the ratio of AP$^-$ cell to AP$^+$ conversion reached up to 70 percent in 4T1 at the single cell level (**Figure 2F**, **2G**). In the hepatic micro-metastasis of 4T1 cells, ES-like cells which were about 5-6 μm in diameter and expressed Oct4 in nucleus could be observed during the derivation of somatic tumor cells from PGC-like cells (**Figure 2H**), indicating that PGC-like cells generated into somatic tumor cells through the similar way to PGC-EGC-somatic cell conversion in testicular teratomas [8]. Taken together, the findings suggest that somatic-PGC-like mutual transformation appears in 4T1 cells.

A crucial role of SPLT formation in tumorigenicity

To validate the crucial role of PGC-like state in the tumorigenicity of 4T1 cells and the similarities of the PGC-like cells with natural PGCs, we knocked out a serial of genes related with PGC specification in 4T1 cells using CRISPR-Cas9, such as embryonic/germ cell related gene Oct4, Sox2, Nanog or PRDM14 as well as germ cell specific genes DDX4 or DAZL [34, 36]. Upon knockout of any one of these genes, the formation of PGC-like cells was impaired abruptly (**Figure 3A**), indicating that the formation of PGC-like cells is likely maintained by a gene network regulating the nature PGCs [34, 36]. At the single cell level, the efficiency of SPLT was decreased abruptly in 4T1-KO group versus 4T1-control group (**Figure 3B**). To further validate the critical role of SPLT in tumorigenicity, we subcutaneously injected these knockout cells into mice. Inhibition of SPLT by knockout of any one of the genes in 4T1 cells abrogated

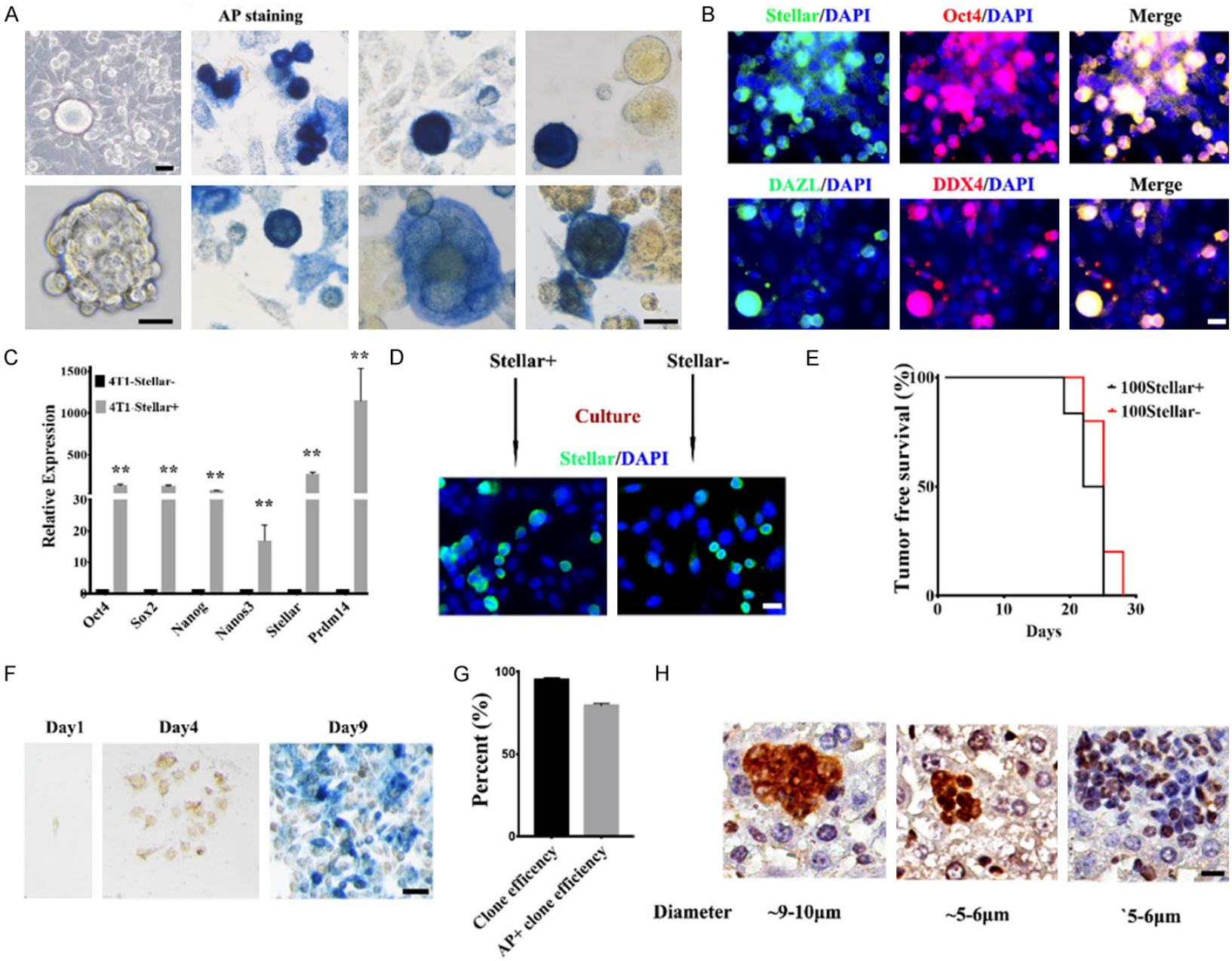
A
AP staining
B
Stellar/DAPI
Oct4/DAPI
Merge
DAZL/DAPI
DDX4/DAPI
Merge
C
4T1-Stellar-
4T1-Stellar+
Relative Expression
Oct4
Sox2
Nanog
Nanos3
Stellar
Prdm14
D
Stellar+
Stellar-
Culture
Stellar/DAPI
E
100Stellar+
100Stellar-
Tumor free survival (%)
Days
F
Day1
Day4
Day9
G
Percent (%)
Clone efficency
AP+ clone efficiency
H
Diameter
~9-10μm
~5-6μm
`5-6μm

Figure 2. Appearance of somatic cell-to-PGC like transfor-mation in 4T1 cells. (A) Bright field image of germ cell-like cells and pre-implantation embryo-like structures with or without AP staining. (B) The immunofluorescence showed 4T1culturs stained with indicated antibodies. (C) qRT-PCR showed the expression of indicated genes in 4T1 stellar$^+$ or Stellar cells. (D) Both 4T1 stellar$^+$ and Stellar cells generated offspring containing stellar$^+$ and Stellar cells. (E) The tumor-free survival curve showed the tumor initiation potential in 4T1 stellar$^+$ or Stellar cells. (F) Derivation of clone with AP$^+$ cells from AP$^-$ cells at single cell level. (G) The efficiency of clones and clones with AP$^+$ round cells in 4T1 cells at single level within a month. (H) In the hepatic micro-metastasis of 4T1 cells, smaller round cells resembling ES cells which was ~5-6 μm in diameter and expressed Oct4 in nucleus could be observed during the derivation of somatic tumor cells from PGC-like cells (~9-10 μm in diameter). Scale bar = 10 μm (H), 20 μm (A, B, D), 50 (F). $^{**}P < 0.01$, $^{****}P < 0.0001$.

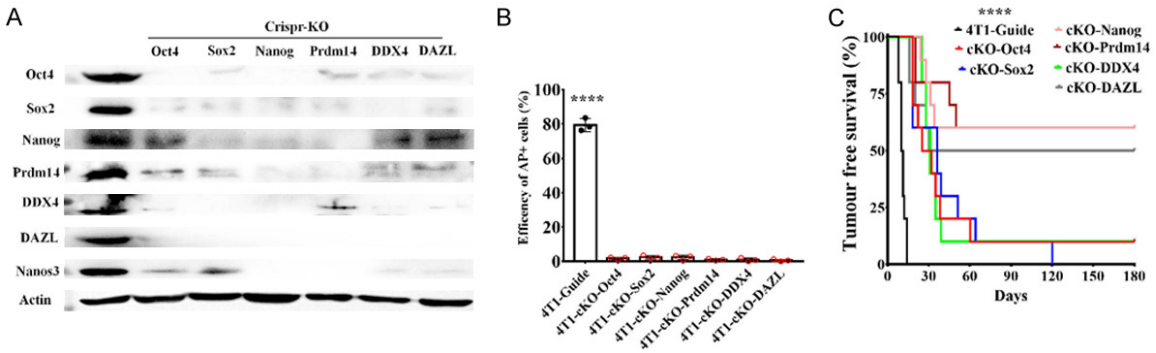

Figure 3. A crucial role of PGC-like cell formation in tumor initiation of 4T1 cells. A. WB results of indicated proteins in 4T1 cultures with different knockout gene. B. The plot shows the formation efficiency of AP-positive cells in 4T1 cells with different knockout gene versus 4T1 control cells. C. The tumor-free survival curve showed the difference of 4T1 cells with different knockout gene and 4T1 control cells in tumor initiation potential.

tumor initiating potential (**Figure 3C**). Thus, obtaining the SPLT is essential for tumorigenicity of 4T1 cells, and SPLT is governed by a serial of PGC development-related genes. It is possible that the breakdown of SPLT might be a potential strategy for cancer therapy.

PGC specification pathway orchestrates SPLT

PGC specification is viewed as the first and perhaps most critical event in germ cell development. It was documented that BMP pathway is essential for governing PGC specification [34, 37]. We then investigated whether the pathway of PGC specification regulates the SPLT. We found that DMH2, an inhibitor of activin A receptor type I (Acrv1), which is an essential receptor of BMP pathway in PGC specification, markedly suppressed proliferation and PGC-like cell formation in 4T1 cultures in a dose-dependent manner (**Figure 4A**, **4B**). Upon treatment with 8 μM DMH2 for 48 h, the AP$^+$ cells were barely observed in 4T1 cultures (**Figure 4B**). Consistently, the results of WB showed that DMH2 inhibited the Smad1/Smad5 signal pathway [38] (**Figure 4A**) which is the key regulator of PGC specification, accompanied by impairing the expression of embryonic/germ cell related genes and germ cell specific genes (**Figure 4A**). Of note, the removal of the DMH2 restored the SPLT in 4T1 cells (**Figure 4B**). Alteration of gene expression related to PGC specification during the course of DMH2 treatment is correlated with the formation of PGC-like cells (**Figure 4C**). After treated with 8 μM DMH2 for 48 h, the 4T1 cultures were injected into mice. The animal data showed that the DMH2 treated group versus control group displayed the similar tumorigenicity potential (**Figure 4D**), consistent with the fact that SPLT state was restored after DMH2 removal. The findings indicated that BMP pathway, a core pathway of PGC specification [34, 37], might be a master regulator in SPLT.

To further validate the crucial role of BMP pathway, we then investigated the role of the BMP pathway, such as Acrv1 and Smad1/Smad5 in the SPLT of 4T1 cells [34, 37]. After deleting the Acvr1, Smad1 or Smad5 with CRIPR-Cas9 technology, the 4T1 cells displayed the impaired PGC-like cell formation (**Figure 4E-H**). Consistently, the data of RT-PCR showed that the genes related to PGC specification

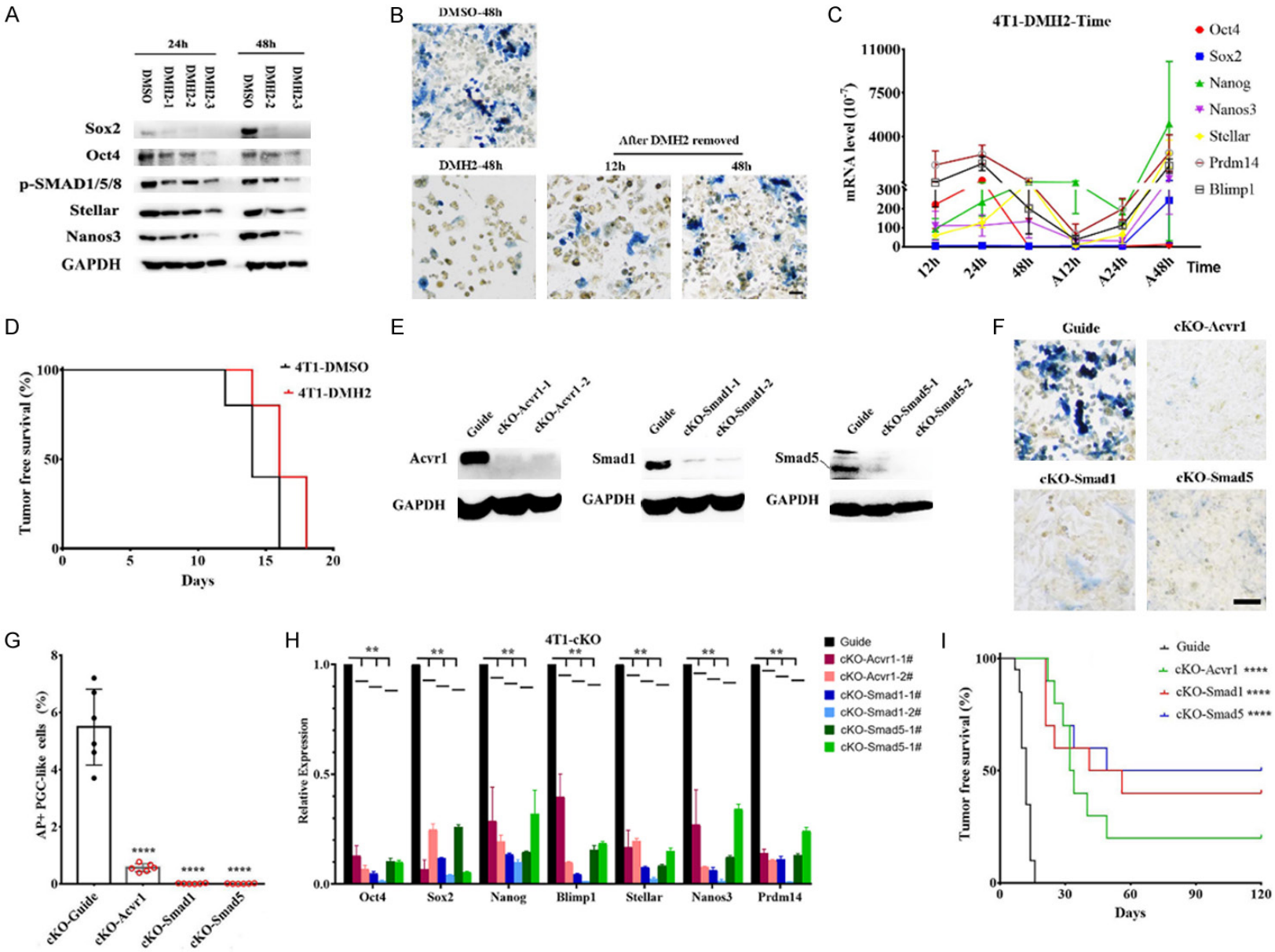
A
24h
48h
DMSO
DMH2-1
DMH2-2
DMH2-3
DMSO
DMH2-2
DMH2-3
Sox2
Oct4
p-SMAD1/5/8
Stellar
Nanos3
GAPDH
B
DMSO-48h
DMH2-48h
After DMH2 removed
12h
48h
C
4T1-DMH2-Time
mRNA level (10^-7)
11000
7500
4000
300
200
100
0
12h
24h
48h
A12h
A24h
A48h
Time
Oct4
Sox2
Nanog
Nanos3
Stellar
Prdm14
Blimp1
D
Tumor free survival (%)
100
50
0
0
5
10
15
20
Days
4T1-DMSO
4T1-DMH2
E
Guide
cKO-Acvr1-1
cKO-Acvr1-2
Acvr1
GAPDH
Guide
cKO-Smad1-1
cKO-Smad1-2
Smad1
GAPDH
Guide
cKO-Smad5-1
cKO-Smad5-2
Smad5
GAPDH
F
Guide
cKO-Acvr1
cKO-Smad1
cKO-Smad5
G
AP+ PGC-like cells (%)
8
6
4
2
0
****
****
****
cKO-Guide
cKO-Acvr1
cKO-Smad1
cKO-Smad5
H
4T1-cKO
Relative Expression
1.0
0.5
0.0
**
Oct4
Sox2
Nanog
Blimp1
Stellar
Nanos3
Prdm14
Guide
cKO-Acvr1-1#
cKO-Acvr1-2#
cKO-Smad1-1#
cKO-Smad1-2#
cKO-Smad5-1#
cKO-Smad5-1#
I
Tumor free survival (%)
100
50
0
0
30
60
90
120
Days
Guide
cKO-Acvr1 ****
cKO-Smad1 ****
cKO-Smad5 ****

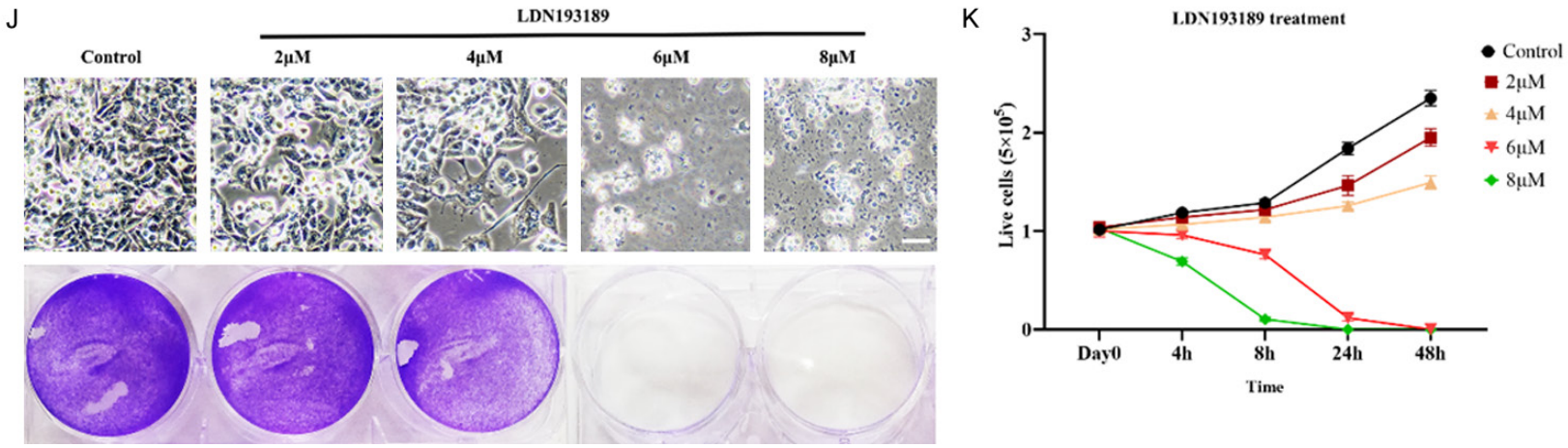

Figure 4. Roles of BMPs pathway in the tumorigenicity of 4T1 cells. (A) WB results of indicated proteins in 4T1 cultures treated with DMSO (control) or DMH2 at different time points. The concentration of DMH2-1, DMH2-2 and DMH2-3 was 3 μM, 6 μM and 8 μM respectively. (B) Bright field image of AP^+ germ cell-like cell formation in 4T1 cultures treated with DMSO (control) or DMH2 at different time point. (C) The mRNA level of indicated genes versus GAPDH in 4T1 cell cultures treated with DMH2 (8 μM) at the different time points and after DMH2 removal. (D) The survival curve of tumor-free cells showed tumor initiation potential in 4T1 cultures treated with DMSO (control) or DMH2 (8 μM) for 48 h. (E) WB results showed that indicated proteins expressed in 4T1 cultures with control or indicated gene knockout. (F) AP staining of 4T1 cultures with control or knockout of indicated genes. (G) The percentage of AP^+ PGC-like cells in 4T1 cells with control or indicated gene knockout. (H) The mRNA level of indicated genes in 4T1 cultures with control or indicated gene knockout. (I) The survival curve of tumor-free cells showed the difference between 4T1-control and 4T1-KO indicated gene in the ability of tumor initiation. (J) The viable cells (under the microscope or stained with crystal violet) of 4T1 cultures after treatment with PBS (control) or LDN193189 for 48 h. (K) Quantification of viable cells over time after treatment with LDN193189 at different time points in 4T1 cultures. Error bars represent ± SEM of three replicate experiments. Scale bar = 50 μm (B, F, J). $^{**}P < 0.01$, $^{****}P < 0.0001$.

decreased robustly after knockout of Acvr1, Smad1 or Smad5 (**Figure 4H**). The efficiency of SPLC was decreased abruptly in 4T1-KO group versus 4T1-control group (**Figure 4F-H**). As a result, the 4T1-KO group showed abrupt decline in tumor initiating potential compared with 4T1-control group (**Figure 4I**). Consistent with this, LDN193189 (BMP type I receptor blocking agent [33], BMP type I receptor which plays a key role in PGC specification [34]) suppressed the growth of 4T1 cells (**Figure 4J**, **4K**). Notably, all the 4T1 cells were killed after treatment with 8 μM LDN193189 for 24 hours or 6 μM LDN193189 for 48 hours (**Figure 4J**, **4K**). These findings further validate that PGC specification pathway [34, 37] governs SPLT, which is essential for tumorigenicity of 4T1 cells.

Roles of Blimp1 in SPLT and tumorigenicity

To further strengthen the concept, we then investigated whether Blimp1, an important downstream target of Smad1/Smad5 serving as one of the core regulators of PGC specification [34, 37], is essential for SPLT. Interestingly, the expression of Blimp1 was higher in 4T1 and T2 than 168FARN and T7 cells (**Figure 1F**, **1I**), which might contribute to distinguish the formation of PGC-like state among the cell lines. Consist with this, the results of immunofluorescence showed that Blimp1 expressed in some of 4T1 cells (**Figure 5A**). There are some cells with both positive for Blimp1 and Prdm14 or Blimp1 and Ifitm3 (**Figure 5A**). Some cells were only positive for Blimp1, Prdm14 or Ifitm3 (an early PGC marker [34]) (**Figure 5A**), indicating that pre-PGC-like cells and PGC-like cells at the different developmental stage existed in the 4T1 cultures. Notably, after deletion of Blimp1 with CRISPR-Cas9, the 4T1 cells showed robust impairment in SPLC and tumorigenicity (**Figure 5B-E**), which further indicated that the downstream of Smad1/Smad5 pathway also regulate the formation of PGC-like cell formation and played a crucial role in the tumorigenicity of 4T1 cells. Together, the findings further indicated that PGC specification governs SPLT and tumor initiation in 4T1 cultures (**Figure 5F**).

Discussion

Our data indicated that acquisition of embryonic/germ cell traits is essential for tumorigenicity. A compelling finding in our study is that tumorigenicity is coupled to the acquisition of PGC-like state through SPLT triggered by the signal pathway involved in PGC specification including Acvr1-Smad1/Smad5-Blimp1 signaling pathway in 4T1 cells, which represent one of aggressive tumor types. In addition, the deletion of any genes related with PGC determination, such as Oct4, Sox2, Nanog, PRDM14, Blimp1, DDX4 and DAZL, inhibited abruptly the formation of PGC-like cells and tumor initiation of 4T1 cells, which provide strong supports for the crucial role of SPLT in tumorigenicity.

Our findings indicated that there might be two distinct ways to gain the tumorigenicity potential from somatic state. The 168FARN cells use one way via reactivation of ES-like state to obtain tumorigenicity without the metastatic capability. Consistent with this finding, ES cells typically exhibit the tumorigenicity but non-invasive [39]. However, the 4T1 cells utilize another way via ES/PGC-like state from somatic state through the activation of SPLT. In this case, the PGC-like state is critical for tumorigenicity and metastasis [19]. Consistence with this, some human tumors showed strong metastatic feature at the beginning, which is even earlier than the time when clinic diagnosis was made [40]. Thus, targeting SPLT appears to be a promising strategy for combating those tumor types resembling 4T1 cells.

Somatic to germ cell transformation naturally occurs in plants and a few animal phyla such as cnidarians, flatworms and tunicates [41]. It also appears spontaneously in the Caenorhabditis elegans strains with long life-span and inactivation of Rb homolog LIN-35 promotes the transformation [37, 42, 43]. Since SPLT can spontaneously happen during cancer progression, it is possible that some somatic cells re-obtain the ability of SPLT through the mechanism yet to be discovered, which then causes the tumor initiation. The activation of PGC-like state in tumors can be facilitated by *p53* deficiency [18, 41] possibly representing aggressive stage, consistent with its essential role in metastasis. In addition, chemical carcinogens, such as (3-methyl-cholanthrene, 3-MCA) [28], also might trigger the SPLT. Therefore, we postulated that the mechanisms underlying SPLT are likely related to many factors linked to tumorigenesis or tumor malignant progression that cause the specification or maintain of PGC-like state from somatic cells. Combined with our previous studies [19, 32] and literatures [41], our find-

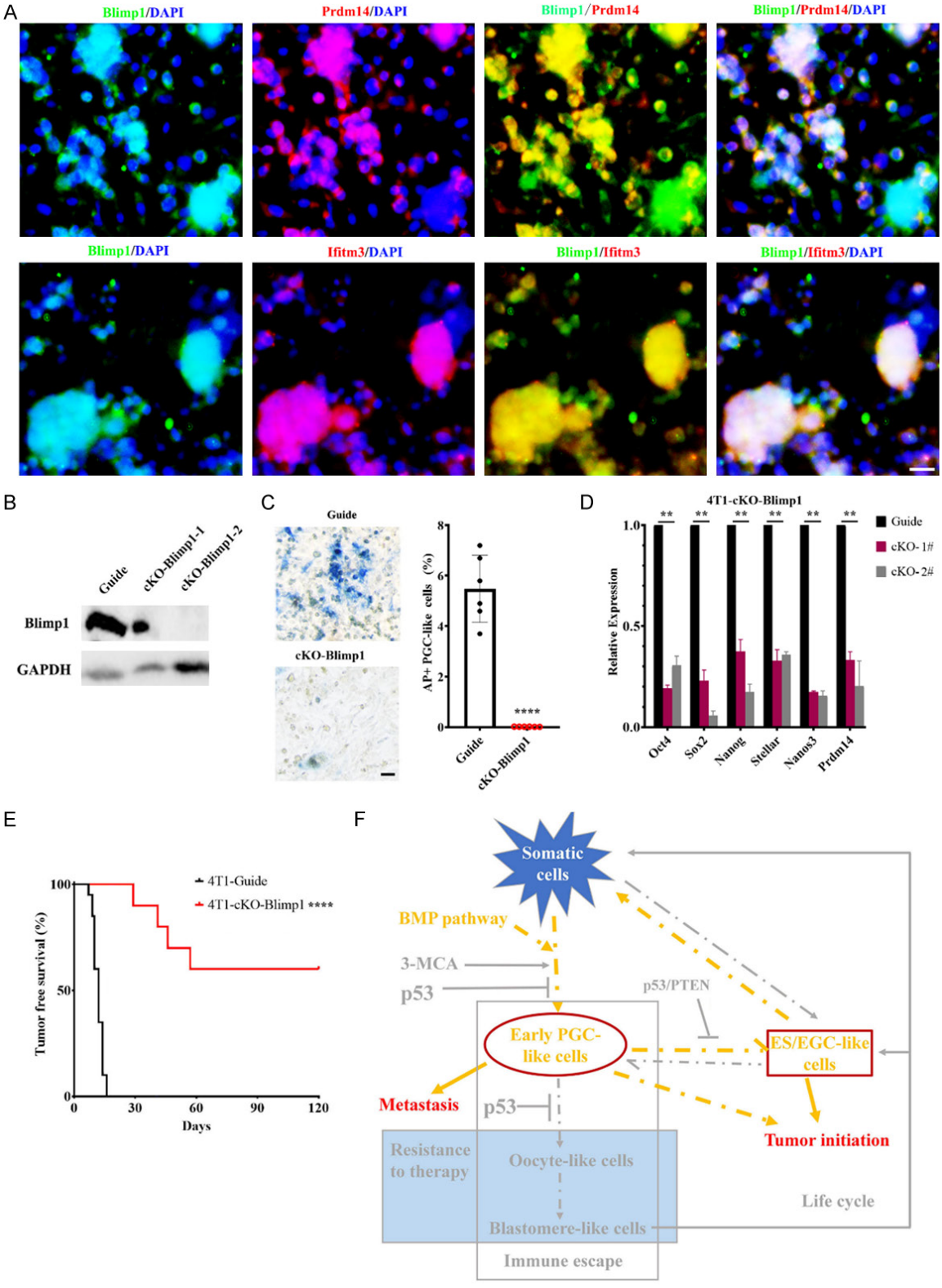

Figure 5. Roles of Blimp1 in tumor initiation of 4T1 cells. (A) The immunofluorescence showed 4T1 cultures stained with indicated antibodies. (B) WB results showed that indicated proteins expressed in 4T1 cultures with control or indicated gene knockout. (C) AP staining of 4T1 cultures with control or knockout of indicated genes (left). The percentage of AP^+ PGC-like cells in 4T1 cells with control or indicated gene knockout (right). (D) The mRNA level of indicated genes in 4T1 cultures with control or indicated gene knockout. (E) The survival curve of tumor-free cells

showed the difference between 4T1-control and 4T1-KO indicated gene in the ability of tumor initiation. (F) The working model of this finding along with the documents and our previous studies. The yellow showed our current findings of 4T1 cells. The grey lines showed conclusion derived from our previous studies [18, 19] or documents [10, 34]. Scale bar = 25 μm (A), 50 μm (C). $^{**}P < 0.01$, $^{****}P < 0.0001$.

ings indicated that embryonic/PGC-like state might be core phenotypes to drive tumor initiation and that PGC-like properties were also associated with metastatic ability (**Figure 5F**). Moreover, the PGC-like tumor cells possibly return to somatic state via the pathways of PGC-EGC like conversion and/or parthenogenetic activation of oocyte-like tumor cells (**Figure 5F**). Therefore, our findings reveal that tumorigenicity is attributed to the acquisition of PGC-like state through SPLT in 4T1 cells but not merely the activation of germ cell-related genes [24], which may enable to deeper understand the biological nature of tumors through embryonal/gametogenesis-related theory of tumors and provide useful targeted strategies for tackling cancer resembling 4T1 cells.

While it still remains a dispute which phenotype links to the central malignant nature of tumors, such as tumorigenicity and metastasis [40, 44], it is widely accepted that tumor is a disease of abnormal growth which is regulated mainly by cell cycle arrest, apoptosis, and senescence [44]. However, targeting abnormal growth is not very efficient for cancer therapy over the last several decades [44]. Moreover, it was reported deficiency of cell cycle arrest, apoptosis and senescence in mice is not sufficient for maintaining spontaneous tumor development [45, 46]. The findings indicated that not only a brake but also a powerful engine like “seed” are needed to drive tumorigenesis. As we know, early PGCs contribute to tumorigenicity and metastasis [6, 34]. Of note, our current study showed that the SPLT can endow somatic cells with the “seed” of tumor initiation, thus providing further supports for the concept that tumor is a disease of abnormal gametogenesis. Thus, our current finding is instrumental to help better understand the nature of tumor biology and likely offers novel strategies and targets for tumor treatment.

Acknowledgements

This work was supported by the Natural Science Foundation of China (No. 82273113), Shanghai Natural Science Foundation of China (No. 21ZR1410900) and Shanghai Municipal Key Clinical Specialty of China (SHSLCZDZK03303). to C.L, start-up funds from Wake Forest University School of Medicine to H.K.L.

Disclosure of conflict of interest

H.K.L. is a consultant for Stablix, Inc. All other authors have declared that no competing interests exist.

Address correspondence to: Chunfang Liu, Department of Laboratory Medicine, Huashan Hospital, Shanghai Medical College, Fudan University, Shanghai 200040, China. E-mail: chunfang_liu@fudan.edu.cn; Huikuan Lin, Department of Cancer Biology, Wake Forest University School of Medicine, Winston-Salem, NC 27157, USA. E-mail: hulin@wakehealth.edu

References

[1] Simpson AJ, Caballero OL, Jungbluth A, Chen YT and Old LJ. Cancer/testis antigens, gametogenesis and cancer. Nat Rev Cancer 2005; 5: 615-625.

[2] Brewer BG, Mitchell RA, Harandi A and Eaton JW. Embryonic vaccines against cancer: an early history. Exp Mol Pathol 2009; 86: 192-197.

[3] Bignold LP, Coghlan BL and Jersmann HP. Hansemann, Boveri, chromosomes and the gametogenesis-related theories of tumours. Cell Biol Int 2006; 30: 640-644.

[4] Old LJ. Cancer is a somatic cell pregnancy. Cancer immun 2007; 7: 19.

[5] Stevens LC. The development of transplantable teratocarcinomas from intratesticular grafts of pre- and postimplantation mouse embryos. Dev Biol 1970; 21: 364-382.

[6] Stevens LC. Origin of testicular teratomas from primordial germ cells in mice. J Natl Cancer Inst 1967; 38: 549-552.

[7] Stevens LC and Little CC. Spontaneous testicular teratomas in an inbred strain of mice. Proc Natl Acad Sci U S A 1954; 40: 1080-1087.

[8] Kimura T, Suzuki A, Fujita Y, Yomogida K, Lomeli H, Asada N, Ikeuchi M, Nagy A, Mak TW and Nakano T. Conditional loss of PTEN leads to testicular teratoma and enhances embryonic germ cell production. Development 2003; 130: 1691-1700.

[9] Thomson JA, Itskovitz-Eldor J, Shapiro SS, Waknitz MA, Swiergiel JJ, Marshall VS and Jones JM. Embryonic stem cell lines derived from human blastocysts. Science 1998; 282: 1145-1147.
[10] Takahashi K and Yamanaka S. Induction of pluripotent stem cells from mouse embryonic and adult fibroblast cultures by defined factors. Cell 2006; 126: 663-676.
[11] Ezeh UI, Turek PJ, Reijo RA and Clark AT. Human embryonic stem cell genes OCT4, NANOG, STELLAR, and GDF3 are expressed in both seminoma and breast carcinoma. Cancer 2005; 104: 2255-2265.
[12] Rudin CM, Durinck S, Stawiski EW, Poirier JT, Modrusan Z, Shames DS, Bergbower EA, Guan Y, Shin J, Guillory J, Rivers CS, Foo CK, Bhatt D, Stinson J, Gnad F, Haverty PM, Gentleman R, Chaudhuri S, Janakiraman V, Jaiswal BS, Parikh C, Yuan W, Zhang Z, Koeppen H, Wu TD, Stern HM, Yauch RL, Huffman KE, Paskulin DD, Illei PB, Varella-Garcia M, Gazdar AF, de Sauvage FJ, Bourgon R, Minna JD, Brock MV and Seshagiri S. Comprehensive genomic analysis identifies SOX2 as a frequently amplified gene in small-cell lung cancer. Nat Genet 2012; 44: 1111-1116.
[13] Guo Y, Liu S, Wang P, Zhao S, Wang F, Bing L, Zhang Y, Ling EA, Gao J and Hao A. Expression profile of embryonic stem cell-associated genes Oct4, Sox2 and Nanog in human gliomas. Histopathology 2011; 59: 763-775.
[14] Son MJ, Woolard K, Nam DH, Lee J and Fine HA. SSEA-1 is an enrichment marker for tumor-initiating cells in human glioblastoma. Cell Stem Cell 2009; 4: 440-452.
[15] Mu P, Zhang Z, Benelli M, Karthaus WR, Hoover E, Chen CC, Wongvipat J, Ku SY, Gao D, Cao Z, Shah N, Adams EJ, Abida W, Watson PA, Prandi D, Huang CH, de Stanchina E, Lowe SW, Ellis L, Beltran H, Rubin MA, Goodrich DW, Demichelis F and Sawyers CL. SOX2 promotes lineage plasticity and antiandrogen resistance in TP53- and RB1-deficient prostate cancer. Science 2017; 355: 84-88.
[16] Boumahdi S, Driessens G, Lapouge G, Rorive S, Nassar D, Le Mercier M, Delatte B, Caauwe A, Lenglez S, Nkusi E, Brohee S, Salmon I, Dubois C, del Marmol V, Fuks F, Beck B and Blanpain C. SOX2 controls tumour initiation and cancer stem-cell functions in squamous-cell carcinoma. Nature 2014; 511: 246-250.
[17] Liu C, Ma Z, Hou J, Zhang H, Liu R, Wu W, Liu W and Lu Y. Germline traits of human hepatoblastoma cells associated with growth and metastasis. Biochem Biophys Res Commun 2013; 437: 120-126.
[18] Liu C, Cai Z, Jin G, Peng D, Pan BS, Zhang X, Han F, Xu X and Lin HK. Abnormal gametogenesis induced by p53 deficiency promotes tumor progression and drug resistance. Cell Discov 2018; 4: 54.
[19] Liu C, Ma Z, Cai Z, Zhang F, Liu C, Chen T, Peng D, Xu X and Lin HK. Identification of primordial germ cell-like cells as liver metastasis initiating cells in mouse tumour models. Cell Discov 2020; 6: 15.
[20] Moriya C, Taniguchi H, Miyata K, Nishiyama N, Kataoka K and Imai K. Inhibition of PRDM14 expression in pancreatic cancer suppresses cancer stem-like properties and liver metastasis in mice. Carcinogenesis 2017; 38: 638-648.
[21] Chen CL, Uthaya Kumar DB, Punj V, Xu J, Sher L, Tahara SM, Hess S and Machida K. NANOG metabolically reprograms tumor-initiating stem-like cells through tumorigenic changes in oxidative phosphorylation and fatty acid metabolism. Cell Metab 2016; 23: 206-219.
[22] Zhang F, Liu R, Zhang H, Liu C, Liu C and Lu Y. Suppressing Dazl modulates tumorigenicity and stemness in human glioblastoma cells. BMC Cancer 2020; 20: 673.
[23] Adhikari AS, Agarwal N, Wood BM, Porretta C, Ruiz B, Pochampally RR and Iwakuma T. CD117 and Stro-1 identify osteosarcoma tumor-initiating cells associated with metastasis and drug resistance. Cancer Res 2010; 70: 4602-4612.
[24] Janic A, Mendizabal L, Llamazares S, Rossell D and Gonzalez C. Ectopic expression of germline genes drives malignant brain tumor growth in drosophila. Science 2010; 330: 1824-1827.
[25] Kaufman CK, Mosimann C, Fan ZP, Yang S, Thomas AJ, Ablain J, Tan JL, Fogley RD, van Rooijen E, Hagedorn EJ, Ciarlo C, White RM, Matos DA, Puller AC, Santoriello C, Liao EC, Young RA and Zon LI. A zebrafish melanoma model reveals emergence of neural crest identity during melanoma initiation. Science 2016; 351: aad2197.
[26] Kawamura T, Suzuki J, Wang YV, Menendez S, Morera LB, Raya A, Wahl GM and Izpisua Belmonte JC. Linking the p53 tumour suppressor pathway to somatic cell reprogramming. Nature 2009; 460: 1140-1144.
[27] Yamada Y, Davis KD and Coffman CR. Programmed cell death of primordial germ cells in drosophila is regulated by p53 and the outsiders monocarboxylate transporter. Development 2008; 135: 207-216.
[28] Liu C, Ma Z, Xu S, Hou J, Hu Y, Yu Y, Liu R, Chen Z and Lu Y. Activation of the germ-cell potential of human bone marrow-derived cells by a chemical carcinogen. Sci Rep 2014; 4: 5564.
[29] Liu C, Xu S, Ma Z, Zeng Y, Chen Z and Lu Y. Generation of pluripotent cancer-initiating cells from transformed bone marrow-derived cells. Cancer Lett 2011; 303: 140-149.

[30] Ma Z, Hu Y, Jiang G, Hou J, Liu R, Lu Y and Liu C. Spontaneous generation of germline characteristics in mouse fibrosarcoma cells. Sci Rep 2012; 2: 743.
[31] Ma Z, Liu R, Wang X, Huang M, Gao Q, Lu Y and Liu C. Spontaneous germline potential of human hepatic cell line in vitro. Mol Hum Reprod 2013; 19: 216-226.
[32] Ma Z, Zhang F, Xiong J, Zhang H, Lin HK and Liu C. Activation of embryonic/germ cell-like axis links poor outcomes of gliomas. Cancer Cell Int 2022; 22: 371.
[33] Yum MK, Han S, Fink J, Wu SS, Dabrowska C, Trendafilova T, Mustata R, Chatzeli L, Azzarelli R, Pshenichnaya I, Lee E, England F, Kim JK, Stange DE, Philpott A, Lee JH, Koo BK and Simons BD. Tracing oncogene-driven remodelling of the intestinal stem cell niche. Nature 2021; 594: 442-447.
[34] Saitou M and Yamaji M. Primordial germ cells in mice. Cold Spring Harb Perspect Biol 2012; 4: a008375.
[35] Takahashi K, Tanabe K, Ohnuki M, Narita M, Ichisaka T, Tomoda K and Yamanaka S. Induction of pluripotent stem cells from adult human fibroblasts by defined factors. Cell 2007; 131: 861-872.
[36] Strome S and Lehmann R. Germ versus soma decisions: lessons from flies and worms. Science 2007; 316: 392-393.
[37] Strome S and Updike D. Specifying and protecting germ cell fate. Nat Rev Mol Cell Biol 2015; 16: 406-416.
[38] Goumans MJ, Valdimarsdottir G, Itoh S, Lebrin F, Larsson J, Mummery C, Karlsson S and ten Dijke P. Activin receptor-like kinase (ALK)1 is an antagonistic mediator of lateral TGFbeta/ALK5 signaling. Mol Cell 2003; 12: 817-828.
[39] Cao F, Li Z, Lee A, Liu Z, Chen K, Wang H, Cai W, Chen X and Wu JC. Noninvasive de novo imaging of human embryonic stem cell-derived teratoma formation. Cancer Res 2009; 69: 2709-2713.
[40] Oskarsson T, Batlle E and Massague J. Metastatic stem cells: sources, niches, and vital pathways. Cell Stem Cell 2014; 14: 306-321.
[41] Liu C, Moten A, Ma Z and Lin HK. The foundational framework of tumors: gametogenesis, p53, and cancer. Semin Cancer Biol 2022; 81: 193-205.
[42] Curran SP, Wu X, Riedel CG and Ruvkun G. A soma-to-germline transformation in long-lived caenorhabditis elegans mutants. Nature 2009; 459: 1079-1084.
[43] Wang D, Kennedy S, Conte D Jr, Kim JK, Gabel HW, Kamath RS, Mello CC and Ruvkun G. Somatic misexpression of germline P granules and enhanced RNA interference in retinoblastoma pathway mutants. Nature 2005; 436: 593-597.
[44] Hanahan D and Weinberg RA. Hallmarks of cancer: the next generation. Cell 2011; 144: 646-674.
[45] Li T, Kon N, Jiang L, Tan M, Ludwig T, Zhao Y, Baer R and Gu W. Tumor suppression in the absence of p53-mediated cell-cycle arrest, apoptosis, and senescence. Cell 2012; 149: 1269-1283.
[46] Valente LJ, Gray DH, Michalak EM, Pinon-Hofbauer J, Egle A, Scott CL, Janic A and Strasser A. p53 efficiently suppresses tumor development in the complete absence of its cell-cycle inhibitory and proapoptotic effectors p21, Puma, and Noxa. Cell Rep 2013; 3: 1339-1345.

Table S1. Primer for QRT-PCR

Gene	Sequence 5'-3'	Size (bp)
mqOct4-F	TCAGGTTGGACTGGGCCTAGT	100
mqOct4-R	GGAGGTTCCCTCTGAGTTGCTT	
mqSox2-F	GAGGGCTGGACTGCGAACT	72
mqSox2-R	TTTGCACCCCTCCCAATTC	
mqNanog-F	GAAATCCCTTCCCTCGCCATC	160
mqNanog-R	CTCAGTAGCAGACCCTTGTAAGC	
mqNanos3-F	TAAGGCTGGATCCCAAACCA	115
mqNanos3-R	GACTCGCCATTGTGTTTGCA	
mqStellar-F	GCAGTCTACGGAACCGCATT	123
mqStellar-R	GGTCTTTCAGCACCGACAACA	
mqBlimp1-F	AGCATGACCTGACATTGACACC	162
mqBlimp1-R	CTCAACACTCTCATGTAAGAGGC	
mGAPDH-F	AAGGGCTCATGACCACAGTC	207
mGAPDH-R	ACACATTGGGGGTAGGAACA	
mPrdm1-F	AAGCCTTTGCATCTCATGCT	97
mPrdm1-R	AGGAAGCCTTTCCCACAAAT	

Table S2. sgRNAs sequences (Sigma)

Ensemble Symbol	Clone ID	chr_start	chr_end	seq target with PAM
Prdm14	MM5000039290	13124392	13124413	GTCAATGCCAGCGAAGTGAAGG
Oct4	MM5000000760	35509180	35509201	GTACACCCAGGCCGACGTGGGG
Nanog	MM5000030442	122711707	122711728	GCTGTGTGCACTCAAGGACAGG
Sox2	MM5000025223	34650483	34650504	ACAGCTACGCGCACATGAACGG
Sox2	MM5000025224	34650099	34650120	CTGTTCTTCTGGTTGCCGCCGG
Ddx4	MM5000020922	112636000	112636021	AGAACACATCTACAACTGGTGG
Dazl	MM5000020903	50289105	50289126	CAAACACCGTTTTTGTTGGAGG
Acvr1	MM5000002095	58479837	58479858	ACACTGCTGGCCTTCACAGTGG
Smad5	MM5000011390	56727534	56727555	GAAAGGAGCGTTGTTGGGTTGG
Smad1	MM5000020027	79356340	79356361	TGGAAAGAGTCTGGGAACGTGG
Blimp1	MM5000029036	44446835	44446856	TTGTCGGGACTTTGCGGAGAGG

Table S3. The primers were used for the Sanger Sequencing of CRSPR-Cas9 knockout

Gene	Sequence 5'-3'
mSOX2	CCTGTTTTTTCATCCCAATTG
mPRDM14	TCCTCTCTAGGGACTGAGGGA
OCT4	CTCTGACAAGTCTGCCTTTCT
DDX4	GGATTTAGTACAAAGGAATCA
DAZL	TGCTTTCAGTTTCAGAGGTAA
NANOG	CTGCCTGCTTGAGTGTCCCA
SMAD5-1#	AGATTTCTCAGGGTTCCACG
SMAD5-2#	AACAAGTGCCTAGTTTTAGA
SMAD1	CTCCCTTTACCTGAGTTCCAG
ACVR1	TGTCAGGAGTCTGGGCATCA
Blimp1	GTGTTCCTTCTGAGCCATTC

Table S4. Sequencing data of knockout cells with CRIPSR-Cas9

	Knock out DNA with CRIPSR-Cas9 technology
4T1-KO-Acvr1-1#	Query 241 AGGTCAACCAGAAACTTTACAtg----tgtgtg---------- 269 Sbjct 58479916 AGGTCAACCAGAAACTTTACATGTGTGTGTGTGAGGGCCTCTCCTGCGGGAACGAGGACC 58479857 Query 270 --tgtgAGGGCC----------TCTCCTGCGGG----AACGAGGAC---CAC-TGT--- 305 Sbjct 58479856 ACTGTGAAGGCCAGCAGTGTTTTTCTTCTCTGAGCATCAACGATGGCTTCCACGTCTACC 58479797 sgRNA ACACTGCTGGCCTTCACAGTGG Del:58 Query 306 ----GGGCTGCTTTCAGGTTTATTAGCAGGGGAAGATGACGTGTAACACCCCGCCGTCAC 361 Sbjct 58479796 AGAAGGGCTGCTTTCAGGTTTATGAGCAGGGGAAGATGACGTGTAAGACCCCGCCGTCAC 58479737 sgRNA AACCTGAAAGCAGCCCTTCTGG
4T1-KO-Acvr1-2#	Query 241 AGGTCAACCAGAAACTTTACAtgtgtgtgtgtgAGGGCCTCTCCTGCGGGAACG------ 294 Sbjct 58479916 AGGTCAACCAGAAACTTTACATGTGTGTGTGTGAGGGCCTCTCCTGCGGGAACGAGGACC 58479857 Query 295 --------AGGCCAGCAGTGTTTTTCTTCTCTGAGCATCAACGATGGCTTCCACGTCTACC 347 Sbjct 58479856 ACTGTGAAGGCCAGCAGTGTTTTTCTTCTCTGAGCATCAACGATGGCTTCCACGTCTACC 58479797 sgRNA ACACTGCTGGCCTTCACAGTGG Del:17 Query 348 AGAA----TGCTTTCTGGTTTATGAGCAGGGGAAGATGACGTGTAAGAccccccGTCAC 403 Sbjct 58479796 AGAAGGGCTGCTTTCAGGTTTATGAGCAGGGGAAGATGACGTGTAAGACCCCGCCGTCAC 58479737 sgRNA AACCTGAAAGCAGCCCTTCTGG
4T1-KO-Smad1-1#	Query 421 CTTCTGGCTCAGTTCCGCAACCTGGGA 447 Sbjct 79356416 CTTCTGGCTCAGTTCCGCAACCTGGGA 79356390 sgRNA: 79356340 TGGAAAGAGTCTGGGAACGTGG 79356361 Del: 127BP Query 448 ACCCTCACTCCCCAACCGGCTCAGACCCGGGCAGCCCTTTTCAGATGCCAGGTCAGAGGG 507 Sbjct 79356262 ACCCTCACTCCCCAACCAGCTCAGACCCGGGCAGCCCTTTTCAGATGCCAGGTAAGAGGG 79356203
4T1-KO-Smad1-2#	Query 361 ttcctgcttc 370 Sbjct 79356482 TTCCTGCTTC 79356473 sgRNA: 79356340 TGGAAAGAGTCTGGGAACGTGG 79356361 Del: 176BP Query 370 ctacctcAACTGTCCTGGCGGCAGCAGCCTAACCTACCTTCACTCCCCAATCAGATCAGA 429 Sbjct 79356297 CTACCCCAACTCTCCTGGCGGCAGCAGCAGCACCTACCCTCACTCCCCAACCAGCTCAGA 79356238
4T1-KO-Smad5-1#	Query 422 CCAAC----------CAACCCCCATCCTTTTTCCCTTGC 450 Sbjct 56727534 CCAACCCAACAACGCTCCTTTCCCCTTATCTCCTAACAGCCCCTATCCTCCTTCCCCTGC 56727593 sgRNA GAAAGGAGCGTTGTTGGGTTGG Del: 31BP


4T1-KO-Smad5-2#
Query 90 TAGGAGATAAGGGGAAAGGAGCGTTGTTGG--TGGAGGAAA---TCGTCAAACGTGGCGT 144
Sbjct 56727568 TAGGAGATAAGGGGAAAGGAGCGTTGTTGGGTTGGTGGAAAGAATCGGGAAACGTGGCGT 56727509
sgRNA: GAAAGGAGCGTTGTTGGGTTGG Del: 5BP
4T1-KO-Blimp1-1#
Query 181 TGCCAACCAGGAACTTCTTGTGTGG 205
Sbjct 44446883 TGCCAACCAGGAACTTCTTGTGTGG 44446859
sgRNA: 44446839TTGTCGGGACTTTGCGGAGAGG Del: 188BP
Query 202 GTGGCTTTAGCTAAAACGAGGAAGAGGAAAAACATTCTTTAATGTCCCTACTTCTTATTA 261
Sbjct 44446666 GTGGCTTTAGCTAAGACGAGGAAGAGGAAAAACATTCTTTAATGTCCCTACTTCTTATTA 44446607
4T1-KO-Blimp1-2#
Query 184 GCCAACCAGGAACTTCTTGTGTGGTAT----------GGCTCCACTACCCT 224
Sbjct 44446882 GCCAACCAGGAACTTCTTGTGTGGTATTGTCGGGACTTTGCGGAGAGGCTCCACTACCCT 44446823
sgRNA: TTGTCGGGACTTTGCGGAGAGG Del: 19BP
4T1-KO-Sox2-1#
Query 60 GGCCGTGCACGCCGAGGCCCCCGCCCGC 87
Sbjct 34650293 GGCCGTGCACGCCGAGGCCCCCGCCCGC 34650320
sgRNA: 34650483 ACAGCTACGCGCACATGAACGG Del:799
Query 98 GCTGGGCTCCATGGGCTCTGTGGTCAAGTCCGAGGCCAGCTCCAGccccccGTGGTTAC 157
Sbjct 34651129 GCTGGGCTCCATGGGCTCTGTGGTCAAGTCCGAGGCCAGCTCCAGCCCCCCCGTGGTTAC 34651188
4T1-KO-Sox2-2#
sgRNA: 34650483 ACAGCTACGCGCACATGAACGG Del: big fragment
Query 9 CGGAGGCTTGCTGG-CCCCGGCGGGAACAGCATGGCGAGCGGGGTTGGGGTGGGCGCCGG 67
Sbjct 34650805 CGGAGGCTTGCTGGCCCCCGGCGGGAACAGCATGGCGAGCGGGGTTGGGGTGGGCGCCGG 34650864

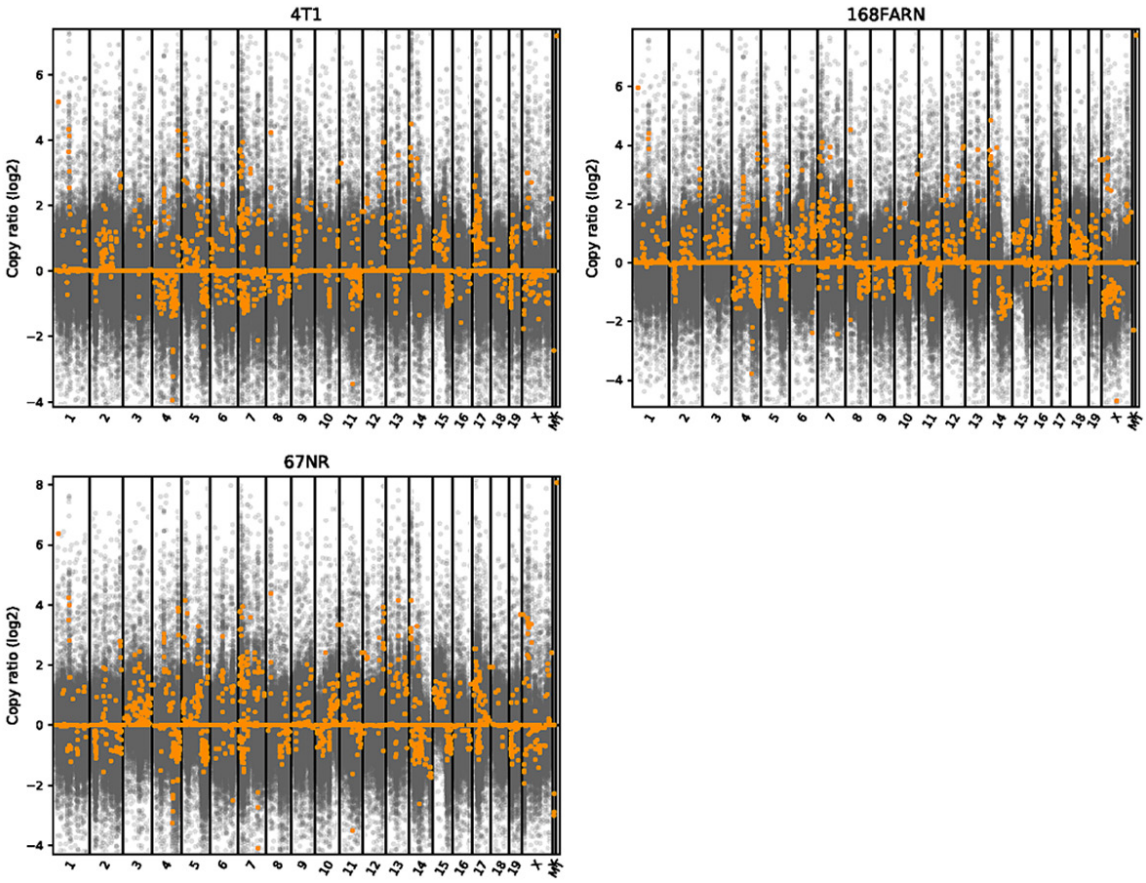

Figure S1. DNA sequencing data showed the copynumber variation of genes among 4T1, 168Farn and 67NR cells.

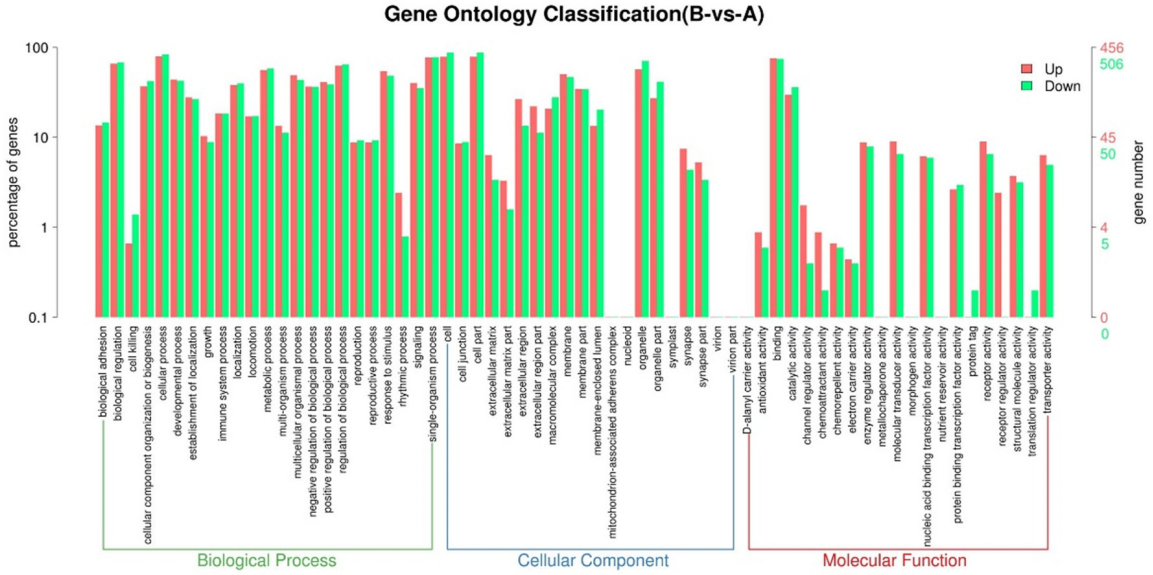
Gene Ontology Classification(B-vs-A)
percentage of genes
gene number
Up
Down
Biological Process
Cellular Component
Molecular Function

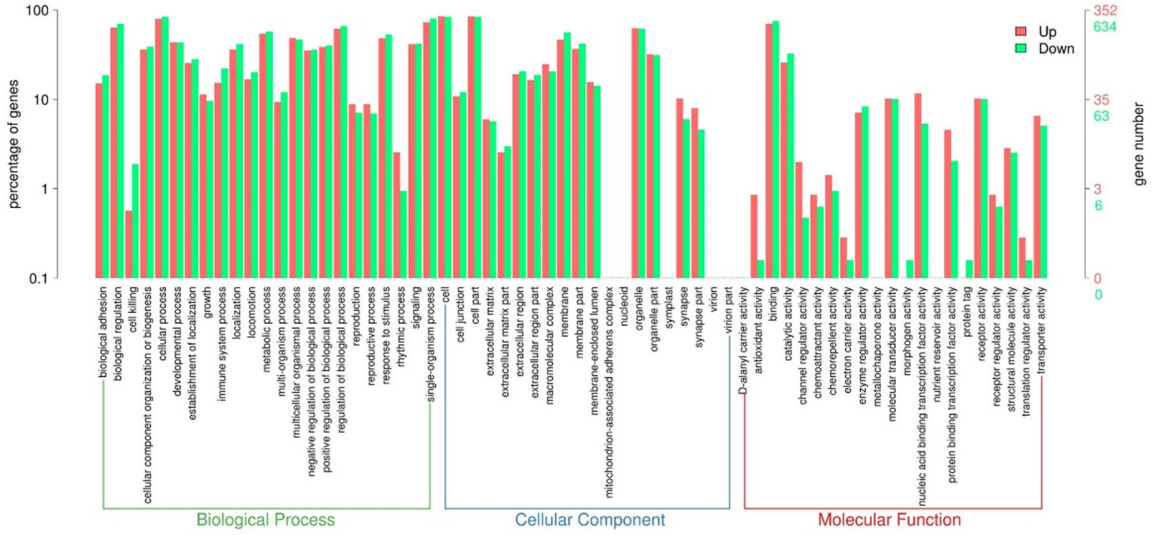
Gene Ontology Classification(C-vs-A)
percentage of genes
gene number
Up
Down
Biological Process
Cellular Component
Molecular Function

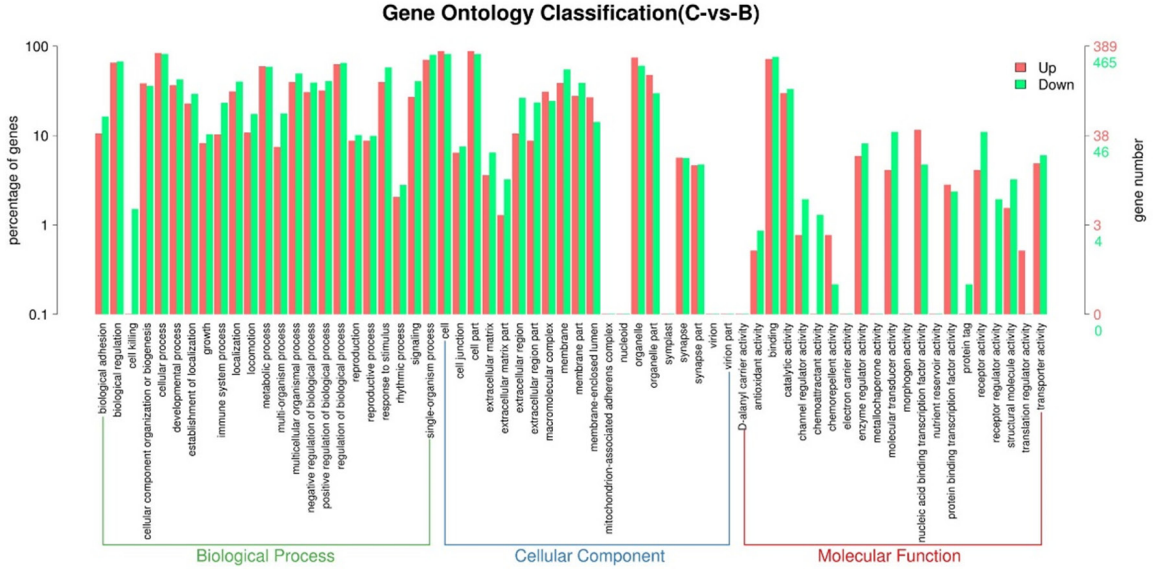
Gene Ontology Classification(C-vs-B)
percentage of genes
gene number
Up
Down
Biological Process
Cellular Component
Molecular Function

Figure S2. RNA sequencing data showed the difference of gene expression among 4T1 (A), 168Farn (B) and 67NR (C) cultures.

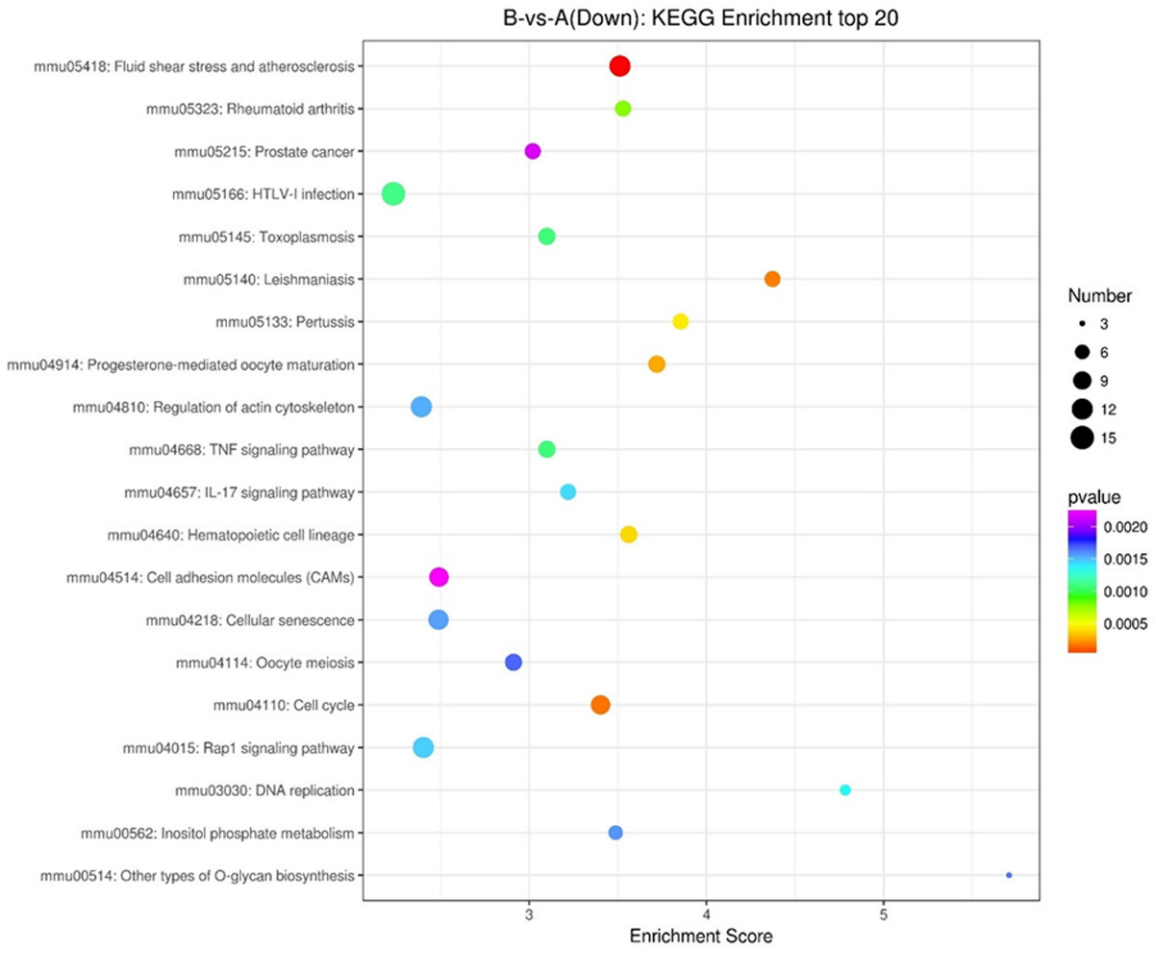

Figure S3. RNA sequencing data showed the top decrease of function gene expression in 168Farn (B) versus 4T1 (A) and and 67NR cultures.

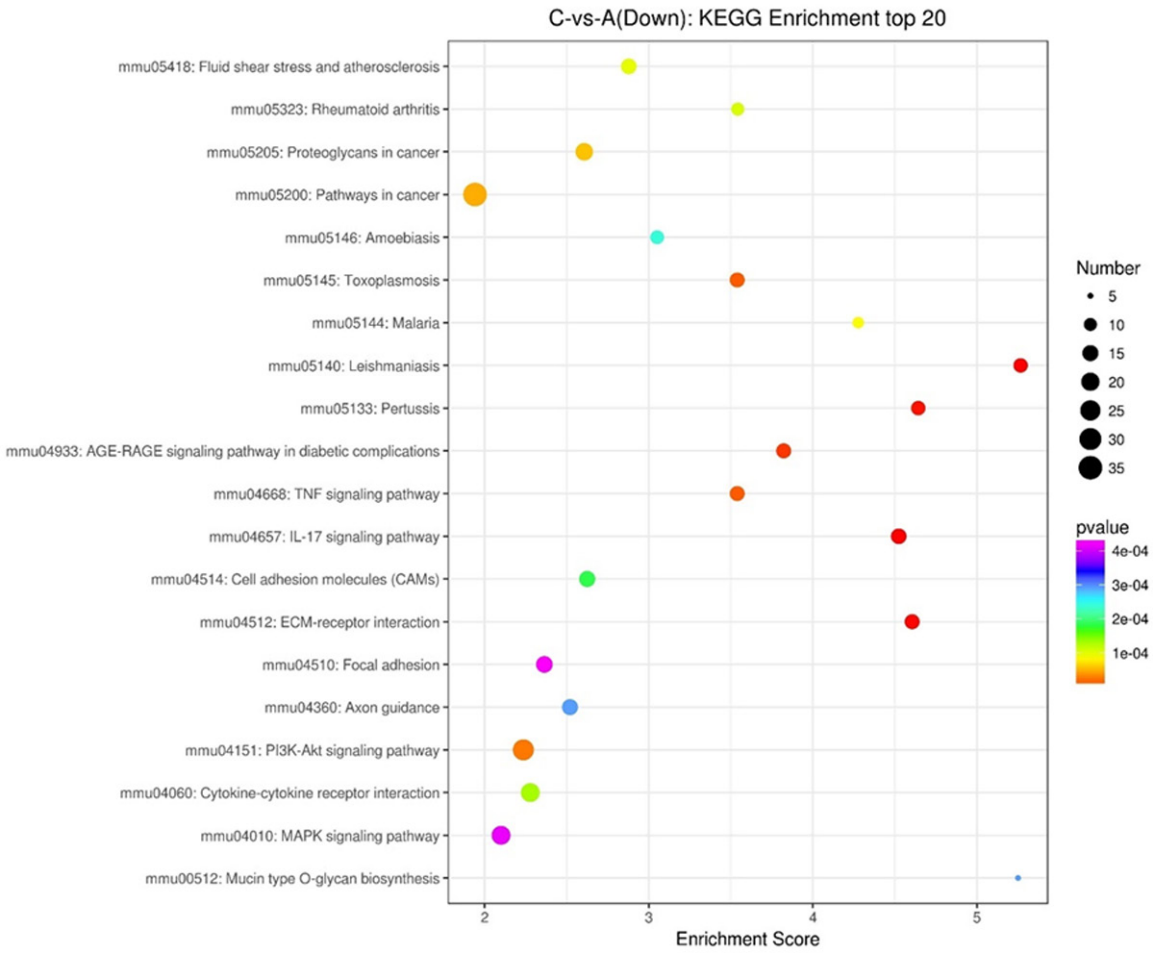

Figure S4. RNA sequencing data showed the top decrease of function gene expression in 67NR (C) versus 4T1 (A) cultures.

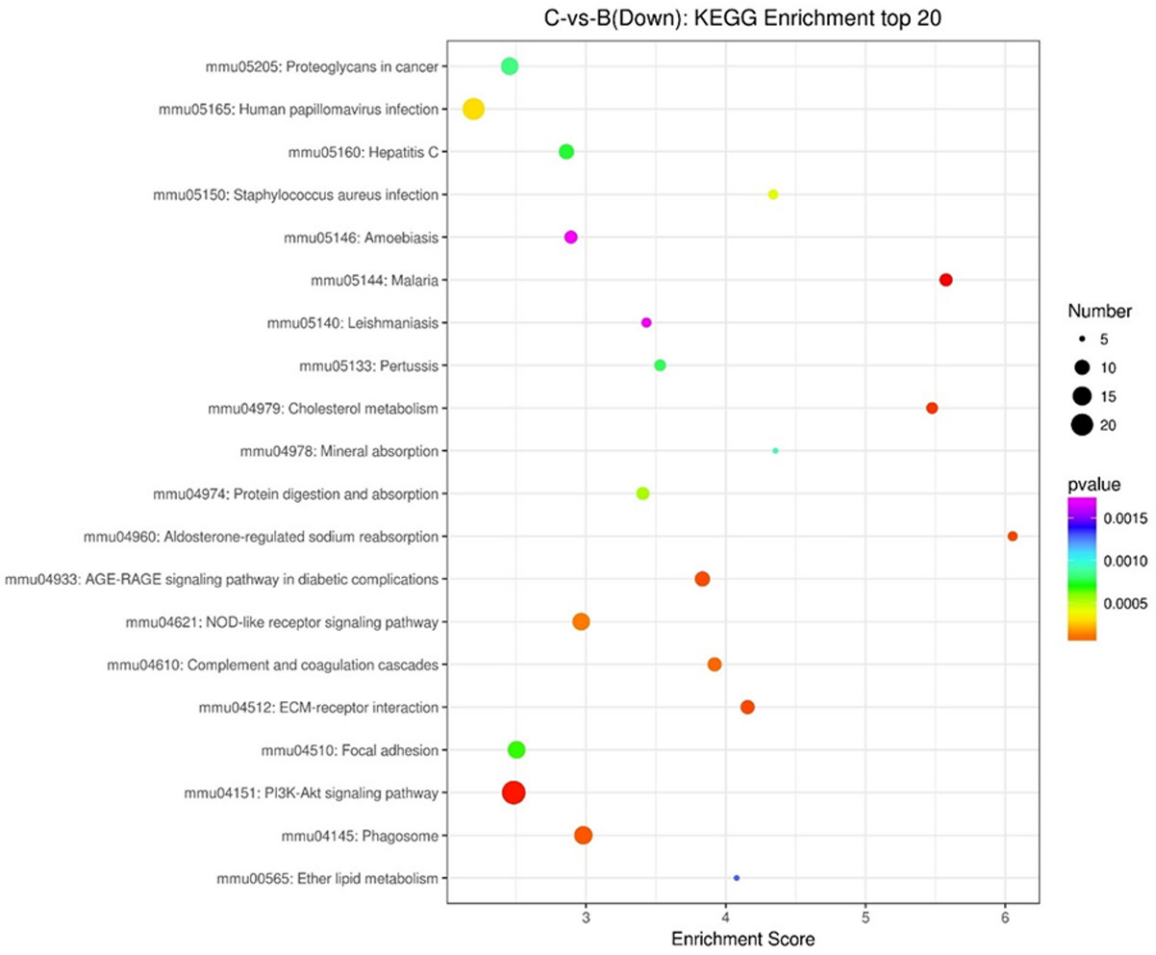

Figure S5. RNA sequencing data showed the top decrease of function gene expression in 67NR (C) versus 168Farn (B) cultures.

Table S5. DNA sequencing data showed the copynumber variation of chromosome with Sox2 gene

chromosome	start	end	gene	log2	cn	depth	probes	type
3	32635926	35675932	Sox2	0.33	3	15.19	131	gain